On the Electron Affinity of Nitromethane (CH_3NO_2)

ARTICLE *in* THE JOURNAL OF PHYSICAL CHEMISTRY A · FEBRUARY 2010

Impact Factor: 2.69 · DOI: 10.1021/jp9113317 · Source: PubMed

3 AUTHORS, INCLUDING:

James N. Bull
University of Melbourne
23 PUBLICATIONS **76** CITATIONS

SEE PROFILE

On the Electron Affinity of Nitromethane (CH_3NO_2)

James N. Bull, Robert G. A. R. Maclagan,* and Peter W. Harland

Department of Chemistry, University of Canterbury, Private Bag 4800, Christchurch 8140, New Zealand

Received: November 29, 2009; Revised Manuscript Received: January 5, 2010

A high-level systematic computational study is presented on an accurate value for the adiabatic valence electron affinity of nitromethane, CH_3NO_2, to resolve literature disagreements in theoretical and experimental reported values. Density functional methods with triple-ζ quality basis sets gave good fortuitous agreement to early experimental determinations, while single-reference wave function based methods employing up to CCSD(T) gave poor or fortuitous agreement depending on the experimental reference value. DFT methods in general cannot accurately describe electron attachment from the result of unphysical self-interaction. It is found that multireference methods with aug-cc-pVTZ or similar basis sets are required to converge to an experimental value. Our highest level of theory 3S-MCQDPT2 and 7S-MCQDPT2 calculations with an aug-cc-pVTZ quality basis description yield values of 0.188 and 0.176 eV (0.170 eV with polynomial extrapolation), in excellent agreement with the most recent experimental value of 0.172 ± 0.006 eV. CCSD(T)//aug-cc-pVTZ provides a fortuitously reasonable description. The isolated dipole-bound anion binding energy is tentatively calculated to be 7−8 meV.

Introduction

Nitromethane, CH_3NO_2, is the simplest alkyl species containing the nitro ($-NO_2$) functional group. It is known to possess a small positive adiabatic valence electron affinity, EA_{ad}, and form a dipole-bound anion where an electron is captured at the positive end of the dipole field with little geometrical rearrangement from the neutral.[1,2] In the gas phase, formation of the valence anion, $CH_3NO_2^-$, was first observed and characterized through collisions of Rydberg-excited Ar and Kr atoms.[3] There have subsequently been six experimental attempts to determine the electron affinity, albeit one a redetermination of existing data.[1,4−8] The new data have resulted in disagreements in the literature on a definitive experimental value, as outlined in Table 1.

The experimental data for the electron affinity of CH_3NO_2 can be arranged into two groups, four averaging 0.47 eV, all within respective experimental errors, and two at 0.26 ± 0.08 and 0.172 ± 0.006 eV, the latter being the most recent determination. The former of these two involved extrapolation of a photoelectron vibrational progression to the last resolvable spectral peak, with this value appearing to be that most widely cited and employed in subsequent calculation at this time. The uncertainty, ranging 180−340 meV, was assigned to allow for one further nonresolvable spectral peak. This value has been suggested to possibly represent an excited state of the anion.[7] The most recent value of 0.172 ± 0.006 eV involved low-energy (higher resolution) photoelectron imaging spectroscopy in an attempt to resolve congestion at the band head. Photoelectron methods are in general not ideally suited to adiabatic measurements but are very well suited to measurement of vertical electron processes, which are the most intense spectral peaks in a full progression. All reported experimental values include errors that in major part do not overlap the two groups. In this paper, we report a series of high level single-reference and multireference calculations to resolve this inconsistency and the apparent lack of convergence of supporting ab initio calculations.

TABLE 1: Summary of Experimental Adiabatic Valence Electron Affinity Determinations, in eV, for CH_3NO_2, Existing in Two Discrete Groupings

experimental technique	EA_{ad}
crossed molecular beam thresholds[a,4]	0.44/0.35 ± 0.20
steady-state electron capture[5]	0.45 ± 0.08
pulse high-pressure EI-MS[6]	0.49 ± 0.11
steady-state electron capture redetermination[7]	0.50 ± 0.10
laser photodetachment photoelectron spectroscopy[b,1]	0.26 ± 0.08
velocity map photoelectron imaging[b,8]	0.172 ± 0.006

[a] Two experimental values correspond to use of different alkai metal charge-transfer reagents, with the larger error incorporating both values. [b] Performed under collision geometry relaxation conditions.

From a theoretical viewpoint, assuming the Born−Oppenheimer approximation, the adiabatic valence electron affinity, EA_{ad}, for a molecular species, where ΔZPV is the molecular zero point energy correction is given as

$$EA_{ad} = E(\text{neutral}) - E(\text{anion}) - \Delta ZPV$$
$$\Delta ZPV = ZPV(\text{anion}) - ZPV(\text{neutral})$$

The most comprehensive previous theoretical investigation of the electron affinity for CH_3NO_2 was carried out by Gutsev et al.,[2,9] where experimental comparison was made *only* to the Compton et al.[1] value of 0.26 ± 0.08. This study was performed using coupled-cluster, and HFDFT methods. Their DFT-type calculation, denoted HFDFT, is a Hartree−Fock density functional theory providing self-interaction density corrections in an attempt to improve anion description.[10] Their findings showed that CCSD (0.055 eV) and CCSD(T) (−0.058 eV) methods with the 6-311++G(d,p) basis set gave very poor agreement, with the latter being negative. Extension to the 6-311++G(2d,2p) basis set improved these by ≈50−60%, yet still in poor agreement with the CCSD value at 0.131 eV. A hybrid basis set designed for identification of dipole-bound states, containing

* Corresponding author. E-mail: robert.maclagan@canterbury.ac.nz.

10.1021/jp9113317
Published on Web 02/15/2010

the addition of seven sp diffuse functions to a 6-311++G(d,p) valence, gave agreement within the lower bound of experimental error with the CCSD (0.192 eV) method, and would apparently be in reasonable agreement with the most recent Adams et al.[8] measurement at 0.172 ± 0.006 eV. Of the basis sets employed, CCSD(T) always yielded values smaller than CCSD counterparts. The HFDFT(B3LYP)//6-311++G(2d,2p)+7sp level of theory yielded reasonable (0.223 eV) but still lower-bound agreement, and MP2 (≤−0.215 eV) methods always performed exceptionally poorly. Surprisingly, their basis set designed to describe the dipole-bound anion provides the apparent closest agreement, yet is not designed to provide a valence description—this may be fortuitous. For a species with a high degree of electron delocalization, we would expect that polarization functions would be important for an accurate description. Further, it must be noted that without ΔZPV corrections, many of these calculations yield negative electron affinities. Three concerns arise: an inadequate valence basis set, shown by the lack of apparent convergence on addition of extra polarization functions; failure of a single-reference wave function to accurately describe the species; comparison with an individual and perhaps incorrect experimental value.

It is useful to first consider nitrogen dioxide, NO_2, which is known to require multiconfigurational wave functions since the $-NO_2$ group orbitals play the dominant role in CH_3NO_2 electron capture, with associated geometrical changes.[2,11,13−16] A Lewis-type interpretation of NO_2 shows resonant charge-separation to preclude each atom from exceeding the octet rule. Acceptance of one electron forms a closed-shell NO_2^- state, completing each atoms octet and yielding a positive valence electron affinity. Alternatively, NO_2 may σ-bond with a methyl radical, $^{\bullet}CH_3$, forming closed-shell CH_3NO_2. Methyl nitrite, or CH_3ONO, is also a stable species and has been calculated to be only ≈2 kcal/mol higher in energy, and in addition, a $HOCH_2NO$ species may exist that has tentatively been calculated to be ≈2 kcal/mol *lower* in energy than CH_3NO_2.[15] Neither of these two latter species are considered here since experimental gas-phase vibrational frequencies for CH_3NO_2 are in excellent agreement with calculations reported herein. Hartree−Fock NO_2 and NO_3 descriptions suffer from symmetry breaking in the wave function where a lower or nearly degenerate energy can be obtained by breaking a higher symmetry.[11,12,16−18] UHF or ROHF[19] wave functions tend to yield orbital localization over resonance, and multiconfigurational wave functions with high levels of static (i.e., large active space) and dynamic electron correlation overcome spatial symmetry breaking and yield a correct description.[18] For NO_2, the nonsymmetry breaking active space has been established to be CASSCF(13,10).[11] Of interest, DFT methods are usually resistant to symmetry breaking, and it has been shown by Sherrill et al.[20] that an increase in the extent of HF exchange (from functional) may promote symmetry breaking. Symmetry breaking considerations for CH_3NO_2 are most likely small; nevertheless, they are ideally considered for the $-NO_2$ group on electron attachment since the anion geometry is significantly different from the neutral, and the O−N−O (Walsh type) bond angle may change with electron detachment.[11]

There have been several previous studies indicating the importance of multiconfigurational wave functions in the accurate description of the $-NO_2$ group in CH_3NO_2 dynamics.[15,20−25] Curve crossings owing to near degeneracy with slight C−N bond stretching of dissociation indicate that π to π^* configurations become more important on electron capture;[20−22] to give reasonable description of $CH_3NO_2 \rightarrow CH_3ONO$ rearrangements;[15] photodynamics and intersystem crossings;[23−25] and anion dissociation dynamics.[14] Calculations have also shown dynamic electron correlation to be important for a description of the neutral,[22] and in accord with NO_2, a CASSCF(14,11) space to be important for wave functions free of symmetry breaking for dissociation. This large active space includes the σ_{CN}^* orbital, which is important for dissociation. The importance of multiconfigurational and dynamical electron correlation has also been shown to be important for CH_3ONO, which readily interconverts with CH_3NO_2.[26] MS-CASPT2 calculations indicate that the closely related anionic CH_3ONO^- species is not stable (negative EA_{ad}),[14] in contrast to the single-reference (inappropriate) MP2 and CC results of Gutsev et al.,[9] which yielded a substantially positive EA_{ad} well above CH_3NO_2 at 0.60 eV HFDFT, 0.27 eV MP2, 0.26 eV CCSD, and 0.30 eV CCSD(T). Arenas et al.[14] also report the highest literature level of theory electron affinity calculation with the internally contracted MS-CASPT2//ANO-L using a CASSCF(15,11) reference to be 0.18 eV with ΔZPV correction. Unfortunately, as discussed below, this ΔZPV correction is incorrect. They also state that removal of f-type polarization reduces the value by ≈0.02 eV, indicating the importance of high-order angular momentum functions in the $-NO_2$ group description. MS-CASPT2 provides systematic improvement of CASPT2 by addition of further CASSCF reference states.[27] All literature calculations mentioned above indicate electron capture to involve a π^* orbital.

Any wave function calculation providing an accurate electron affinity for CH_3NO_2 should therefore be of multiconfigurational nature. Such calculations are very computationally expensive; however, density functional theory (DFT) methods are computationally inexpensive and inherently include some multiconfigurational character. Unfortunately, traditional Kohn−Sham DFT (KSDFT) for anions exhibits unphysical self-interaction altering the energy.[28] In addition, KSDFT employing traditional functionals are known to be less accurate when describing π electrons than for σ electrons.[29] Nevertheless, DFT performance for several common functionals will be evaluated.

Computational Method

All DFT, Møller−Plesset perturbation theory, and coupled cluster calculations have been performed using the Gaussian computational package.[30] All multireference calculations were performed using the GAMESS-US package,[31] as were MP2//aug-cc-pVQZ optimization calculations. [Levels of theory are denoted SP/OPT/BS, where SP denotes the single-point electron correlation method, OPT denotes the optimization electron correlation method (omitted with // if identical to the energy calculation), and BS denotes the basis set used throughout.] Geometrical optimizations and single-point energy calculations at B3LYP geometries were performed for most DFT functionals and single-reference wave function methods, and all multiconfigurational calculations were performed at the B3LYP geometry as outlined later.

The DFT functionals trialed herein are of hybrid or meta-GGA type, which include portions of exact HF exchange to minimize self-interaction. The functionals employed with the extent of exact HF exchange in parentheses are: B3LYP (20%); X3LYP (21.8%); TPSS (0%); TPSSh (10%); from the M06 suite of functionals of Truhlar et al.,[32,33] M06-L (0%), M06 (27%), M06-2X (54%), and M06-HF (100%); and BMK (42%). The BMK functional has been shown to on average perform better than B3LYP and TPSSh.[34] Of the M06 suite, the M06 and M06-2X functionals would be expected to be the most applicable here. In addition, the recent and more comprehensive double-

TABLE 2: Custom Basis Sets for CH_3NO_2 Electron Affinity Determinations

basis set	CH_3 description	NO_2 description
GEN1	aug-cc-pVDZ	aug-cc-pVTZ
GEN2	6-311++G(d,p)	aug-cc-pVTZ
GEN3	aug-cc-pVDZ	aug-cc-pVQZ
GEN4	aug-cc-pVDZ[a]	aug-cc-pVQZ

[a] Carbon atom is treated with aug-cc-pVQZ basis set.

hybrid B2PLYP[34] and MPW2PLYP[35] functions are trialed that include exact HF exchange with MP2 type correlation, and in general outperform B3LYP.

Construction of the CASSCF space follows Schaefer et al.[11] and the detailed description by Arenas et al.[14] Briefly, this involves: C_{1s}, N_{1s}, O_{1s}, O_{2s}, and σ_{CH} as core orbitals, with all remaining occupied orbitals active. The final active space is denoted (14/15,11), where 14/15 denotes the number of neutral/anion electrons, and 11 the number of active orbitals. Wave functions were calculated with C_s point group symmetry.

Dynamical electron correlation is included using the internally uncontracted multiconfigurational quasi-degenerate perturbation theory of second order, NS-MCQDPT2[36] (analogous to MS-CASPT2) method, and when applied to one CASSCF reference state is known as the second-order multireference Møller−Plesset perturbation theory approach (MRMP2).[37] N denotes the number of equally weighted CASSCF configurations, with polynomial extrapolation using 1/N. MRMP2 intruder states arising from quasi-degeneracy are small and removed by denominator level shifting of 0.1 for neutral and anion ground states.[38] High-level MRCI calculations are too expensive for CASSCF references and species of this size.

Four composite basis sets, denoted GEN1 to GEN4 were also constructed to estimate the relative importance of CH_3 and NO_2 groups, by providing a different but systematically better description of both groups. These basis sets are summarized in Table 2.

For dipole-bound calculations, we follow the procedure outlined by Simons et al.,[39,40] calculating the dipole binding energy at the CCSD(T)/aug-cc-pVDZ+6sp7d level of theory. This basis has an aug-cc-pVDZ valence augmented with six additional sp and seven d-type diffuse functions (+6sp7d) centered on the methyl carbon atom. The additional diffuse function orbital exponents start at 7.239×10^{-3} for sp functions and 2.316×10^{-2} for d functions and decrease with an even-tempered geometric progression factor of 3.2. These exponents range the same orders of magnitude as the Gutsev and Bartlett[2] dipole-bound anion study and would minimize linear dependence effects. This additional augmentation is critical to obtain a bound state, where default valence basis sets have an incomplete long-range description. The B3LYP//aug-cc-pVTZ geometry of the neutral is assumed. Simons et al.[39,40] show additional f-type diffuse functions in general are nonbeneficial for similar species, and treating the dipole-bound state with an aug-cc-pVTZ valence yields no gain over the aug-cc-pVDZ valence.

Results and Discussion

A. Geometries. An initial requirement for electron affinity calculations is accurate geometries for both CH_3NO_2 ($^1A'$ ground state) and $CH_3NO_2^-$ ($^2A'$ ground state); however, for the latter there exists no experimental comparison. As a preliminary, we consider NO_2 and NO_2^- optimizations at the B3LYP//aug-cc-pVTZ level of theory, and its ability to reproduce experimental gas-phase anharmonic fundamental vibration frequencies, as summarized in Table 3.

TABLE 3: Experimental and Calculated Gas-Phase Infrared Anharmonic Vibrational Frequencies, in cm^{-1}, for NO_2 and NO_2^- in Parentheses[a]

description	NO_2[b] (NO_2^-)[c,d]	B3LYP
A_1 NO_2 stretch	1318 (1284 ± 30)[c]	1360 (1302)
A_1 NO_2 bend	750 (766 ± 30)[c]	757 (787)
B_2 NO_2 stretch	1618 (1244)[d]	1643 (1252)

[a] Both calculations used the aug-cc-pVTZ basis set. Root-mean-square-displacement (RMSD) for B3LYP//aug-cc-pVTZ values are 25 and 16 cm^{-1} for NO_2 and NO_2^-, respectively, with the individual errors on experimental data for the anion exceeding respective RMSD. [b] Reference 41. [c] Reference 42. [d] Reference 43, measured in argon.

These data show that the dominant vibrational change upon electron capture is a decrease in the NO_2 stretching frequency, corresponding to a bond weakening in support of π^*-type orbital involvement in electron capture. Calculated values are in excellent agreement for both the neutral (open-shell) and anion (closed-shell), indicating the B3LYP//aug-cc-pVTZ level of theory yields accurate geometries for both the neutral and anion. For CH_3NO_2, optimized geometrical bonding parameters at the B3LYP//aug-cc-pVTZ level of theory are shown in Figure 1 and have been previously shown to be in excellent agreement with experiment.[13] The calculated anion geometry also has been shown to be in excellent agreement (third decimal place) with wave function methods.[2,13] Figure 1 shows the dominant geometric change upon electron capture to be an increase of the NO_2 tilt angle, θ. These calculated geometries are also in excellent accord with the B3LYP//6-311++G(2d,p) and CCSD(T)//aug-cc-pVTZ optimizations of Adams et al.,[8] noting they report the NO_2 tilt angles at half their actual value (14.0° and 15.6°, respectively), and in slightly better agreement than at the CASSCF(14,11)//ANO-L level of theory (tilt angle neglected for the neutral, 36.8° anion) with their NO bond length in 0.08 Å poorer agreement to experiment.[24] The CASSCF(14,11)//ANO-L presumably lacks dynamical electron correlation correction to geometries. Calculated gas-phase anharmonic vibrational frequencies for CH_3NO_2 with experimental comparison are reported in Table 4. These data are in excellent agreement with experiment, and also those calculated at the B3LYP//6-311++G(3df,3pd) level of theory,[13] with a root-mean-square displacement of 14 cm^{-1}.

When a species has a small (<1 eV) adiabatic valence electron affinity, and both neutral and anion show different geometries, an accurate ΔZPV correction is required since this may constitute a significant portion of the final value. For CH_3NO_2 this correction is found to be ≈45% of the final value. The anharmonic ΔZPV is calculated to be 0.078 eV at the B3LYP//aug-cc-pVTZ and B3LYP//6-311++G(3df,3pd) levels of theory.[13] These values are slightly larger than the Gutsev and Bartlett[2] MP2//6-311+G(2d,2p) harmonic value of ΔZPV = 0.064 eV. The experimentally determined zero point energy for CH_3NO_2 is 30.28 ± 0.01 kcal/mol,[41] in good agreement with our anharmonic value of 30.72 kcal/mol, and in significantly better agreement than with the value of 31.78 kcal/mol by Gutsev and Bartlett.[2] Adams et al.[8] obtain a harmonic B3LYP//6-311++G(2d,p) ΔZPV = 0.081 eV. Our data indicate that the Gutsev and Bartlett[2] ΔZPV correction is a therefore a slight underestimate.

B. Adiabatic Electron Affinity. To address the concern regarding the basis set in the Gutsev and Bartlett[2] study, we

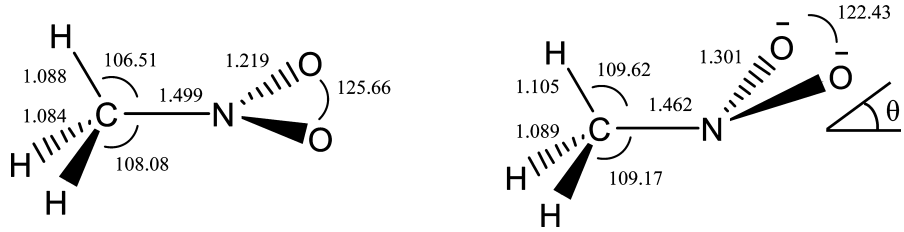

Figure 1. CH_3NO_2 and $CH_3NO_2^-$ B3LYP//aug-cc-pVTZ optimized geometries. $CH_3NO_2^-$−NO_2 tilt angle $\theta = 32.31°$ and 31.55° at the B3LYP//aug-cc-pVTZ and B3LYP//aug-cc-pVQZ levels of theory, respectively. For CH_3NO_2, these are $\theta = 1.64°$ and 1.54°. Reported bond lengths in Å, and angles in degrees.

TABLE 4: Experimental and Calculated Gas-Phase Infrared Anharmonic Fundamental Vibrational Frequencies, in cm^{-1}, for CH_3NO_2 at the B3LYP//aug-cc-pVTZ Level of Theory[a]

description	experimental[b]	calculated
A″ NO_2 rock	475	474
A′ NO_2 wag	603	611
A′ NO_2 scissor	657	645
A′ CN stretch	936	918
A′ CH_3 rock	1096	1088
A′ CH_3 rock	1131	1108
A′ CH_3 deform	1380	1364
A′ NO_2 stretch	1397	1397
A″ CH_3 deform	1410	1421
A′ CH_3 deform	1434	1438
A″ CH_3 stretch	1583	1588
A′ CH_3 stretch	2974	2969
A′ CH_3 stretch	3045	3030
A″ CH_3 stretch	3080	3049
ZPV	30.28 ± 0.01[b]	30.72[c]

[a] Zero point energy (ZPV) in units of kcal/mol. Description of modes follows Gutsev and Bartlett.[2] [b] Reference 44, reality of reported error is tentative. [c] Anion ZPV is calculated at 28.92 kcal/mol.

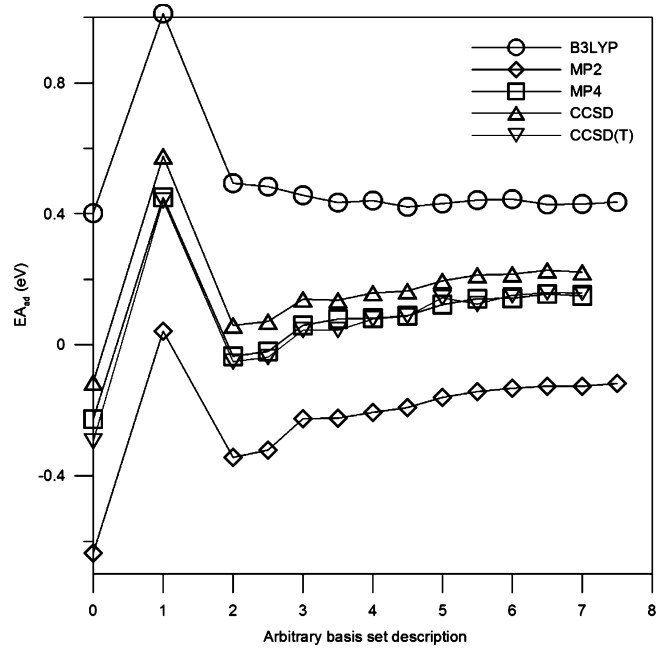

Figure 2. Convergence of basis set to an adiabatic electron affinity (EA_{ad}) in eV for B3LYP, MP2, MP4SDQ, CCSD, and CCSD(T) electron correlation methods. All calculations were performed at the B3LYP//aug-cc-pVTZ geometries with the ΔZPV = 0.078 eV correction. The arbitrary assignment of basis set to a numerical value is described in the text.

performed a series of electron affinity calculations with increasing basis set description using B3LYP, MP2, MP4SDQ, CCSD, and CCSD(T) methods. Each basis set is assigned an ascending arbitrary description number, ranging 0−7.5, representing performance for plotting purposes only. The basis sets employed, with number of Cartesian basis functions in parentheses indicating computational complexity are: 0, 6-311G (61); 1, 6-311++G (80); 2, 6-311++G(d,p) (113); 2.5, 6-311++G(df,pd) (171); 3, 6-311++G(2d,2p) (146); 3.5, 6-311++G(2df,2pd) (204); 4, 6-311++G(3p,3d) (179); 4.5, 6-311++G(3df,3pd) (237); 5, GEN2 (209); 5.5, GEN1 (217); 6, aug-cc-pVTZ (295); 6.5, GEN3 (367); 7, GEN4 (447); 7.5, aug-cc-pVQZ (585). These data are shown in Figure 2 and all assume the B3LYP//aug-cc-pVTZ geometry and ΔZPV correction.

Each electron correlation treatment shown in Figure 2 reveals a sharp positive increase for all correlation methods on initial addition of valence diffuse type (++) basis functions. Such basis functions are well-known to be important for anion states, with these highly positive erroneous EA_{ad} resulting from an overall inadequate valence description. Further diffuse augmentation shows a converging decreasing trend for B3LYP, and a converging increasing trend for wave function based methods. This slow convergence can be assumed to arise with increasing variational freedom as the basis set size increases. The B3LYP calculations show early convergence to a value in agreement with the first set of experimental data, and no significant change as the basis set is increased beyond 6-311++G(3d,3p). In all instances, MP2 yields a negative electron affinity, whereas MP4SDQ yields positive values in good accord with CCSD(T). CCSD values apparently show slow convergence to between the Adams et al.[8] (0.172 ± 0.006 eV) and Compton et al.[1] (0.26 ± 0.08 eV) values, whereas the CCSD(T) value are systematically smaller and appear to converge slowly to approximately the Adams et al.[8] electron affinity. That the CCSD(T) values are systematically smaller in magnitude than the CCSD values may indicate a better description of neutral relative to the anion for CCSD, or the fortuitous agreement of CCSD to the Compton et al.[1] value if correct. Assuming the CCSD(T) method to be more reliable, this data convergence would indicate the Adams et al.[8] value to be correct. Higher-order CCSDT or CCSDTQ would allow much more comprehensive single-reference determinations. That the Gutsev and Bartlett[2] study stated their "best" valence electron affinity determination at 0.192 eV (CCSD) to be with their 6-311++G(d,p)+7sp basis set is most likely reflective of the initial low basis set EA_{ad} jump shown here, where the anion is treated considerably better than the neutral in the absence of adequate polarization type basis functions. That is, their agreement is most likely fortuitous, their additional diffuse functions are designed (without basis set superposition error correction) to describe dipole-bound states off the CH_3-end, not a valence description of the NO_2-end. These data all indicate lack of convergence. Of interest, the GEN1 or GEN3 and aug-cc-pVTZ or GEN4 basis sets yield almost identical values, again indicating the NO_2-group is that which

TABLE 5: Summary of Calculated Adiabatic Electron Affinities, in eV, for CH_3NO_2[a]

level of theory	EA_{ad}
HFDFT(B3LYP)//6-311++G(2d,2p)[b]	0.223
B3LYP//6-311++G(2d,2p)	0.459
B3LYP//aug-cc-pVTZ	0.445
B3LYP//aug-cc-pVQZ	0.436
X3LYP//aug-cc-pVTZ	0.411 (0.411)
TPSS//aug-cc-pVTZ	0.315 (0.317)
TPSSh//aug-cc-pVTZ	0.271 (0.295)
M06-L//aug-cc-pVTZ	(0.024)
M06//aug-cc-pVTZ	(0.211)
M06−2X//aug-cc-pVTZ	0.304 (0.345)
M06-HF//aug-cc-pVTZ	0.595 (0.616)
BMK//aug-cc-pVTZ	0.351 (0.346)
B2PLYP//aug-cc-pVTZ	(0.200)
mPW2PLYP//aug-cc-pVTZ	(0.241)
mPW2PLYP//aug-cc-pVQZ	(0.236)
MP2//aug-cc-pVTZ	−0.126 (−0.133)
MP2//aug-cc-pVQZ	−0.109 (−0.118)
MP4SDQ//aug-cc-pVTZ	(0.143)
CCSD//GEN2	(0.195)
CCSD(T)//GEN2	(0.144)
CCSD//GEN1	(0.213)
CCSD(T)//GEN1	(0.124)
CCSD//aug-cc-pVTZ	(0.216)
CCSD(T)//aug-cc-pVTZ[c]	0.160 (0.150)
CCSD//GEN3	(0.227)
CCSD(T)//GEN3	(0.160)
CCSD//GEN4	(0.221)
CCSD(T)//GEN4	(0.158)
SS-MCQDPT2//aug-cc-pVTZ[d]	(0.286)
SS-MCQDPT2//aug-cc-pVTZ	(0.266)
SS-MCQDPT2//GEN1	(0.266)
2S-MCQDPT2//GEN1	(0.204)
3S-MCQDPT2//GEN1	(0.188)
7S-MCQDPT2//GEN1	(0.178)
MS-CASPT2//ANO-L[e]	0.18/0.24

[a] The values in parentheses are calculated using the B3LYP//aug-cc-pVTZ optimized geometry. All values are corrected using the B3LYP//aug-cc-pVTZ zero point energy correction, $\Delta ZPV = 0.078$ eV. [b] Reference 2 with MP2//6-311+G(2d,2p) harmonic ΔZPV correction. [c] Reference 8 gives an optimized value at 0.162 eV with B3LYP//6-311++G(2df,2p) harmonic ΔZPV correction. [d] Using a CASSCF(14,10) and CASSCF(15,10) reference wave function for neutral and anion respectively. [e] Reference 14 with an erroneous $\Delta ZPV \approx 0.01$ eV correction, the EA_{ad} becomes 0.24 eV with our ΔZPV correction.

is important in electron capture. The GEN1 basis set may therefore provide aug-cc-pVTZ quality description at a significantly lower computational cost for higher electron correlation treatments. Electron affinity determinations on similar species containing the $-NO_2$ group have found that CCSD(T) methods in general underestimate relative to HFDFT methods with the comparative statement "relative insensitivity of density functional theory approaches to augmentations of spd basis sets by functions with higher angular momentum, whereas the convergence of the correlation energy in coupled cluster methods is proportional to $1/L^4$, ... harmonics up to $L = 5$ are required to reach 0.03 eV accuracy".[9] L represents the highest order angular momentum basis function. This same trend has been observed for species employing pentuple-ζ quality bases with iterative triplet coupled cluster corrections.[45] The results of our largest basis set calculated adiabatic electron affinities are reported in Table 5.

The DFT functionals trialed yield a wide range of values spanning all experimental determinations. As expected, B3LYP and X3LYP reproduce each other well, and are apparently in excellent agreement with the higher set of experimental values. The TPSS and M06 suite of functionals show the general trend that as the extent of HF exchange is increased, electron affinities move from being a poor underestimate (0%) to in reasonable agreement with the Compton et al.[1] value (27%), to a poor overestimate (100%). The TPSS, TPSSh, and BMK functionals all yield values between the two groupings of experimental data. The two double hybrid methods yield values between the Compton et al.[1] and Adams et al.[8] values but do perform considerably better than other functionals employing some high degree of HF exchange. Although DFT calculations are inherently multiconfigurational,[28] the large variance for electron affinity calculations here gives skepticism on their use for accurate CH_3NO_2 electron attachment or relative anion energetics. Our data reveals no DFT methods trialed here give reliable agreement to the Adams et al.[8] value. Single-reference wave function calculations all underestimate the Compton et al.[1] value, although as noted above, CCSD(T) shows reasonable agreement with the Adams et al.[8] value. The GEN4 basis set does appear to slightly improve triple-ζ quality description. These single-reference wave function methods would again indicate the higher of the two experimental electron affinity groupings to be incorrect.

TABLE 6: CH_3NO_2 RHF/($CH_3NO_2^-$ ROHF in Parentheses) Wave Function Weights in CASSCF Wave Functions

active space	HF weight
CASSCF(14/15,10)/aug-cc-pVTZ	0.91 (0.96)
CASSCF(14/15,10)/GEN1	0.91 (0.95)
CASSCF(14/15,11)/aug-cc-pVTZ	0.90 (0.93)
CASSCF(14/15,11)/GEN1	0.90 (0.93)

Multiconfigurational ab initio methods do show systematic improvement with an increasing degree of dynamic electron correlation. The most comprehensive multiconfigurational calculation reported is that of Arenas et al.[14] at 0.18 eV, with the MS-CASPT2/CASSCF(14/15,11)/ANO-L level of theory (CASSCF ΔZPV), which appears to be in good agreement with the Adams et al.[8] value. This value is erroneous, as their highly rounded tabulated zero-point energies, presumably from application of an incorrect conversion factor in interpretation of computational output, are systematically an order of magnitude less than our calculated or reported experimental values. As a result, their ΔZPV is incorrect at $\approx$0.01 eV. Application of our ΔZPV correction to the tabulated MS-CASPT2 energies then gave 0.246 eV, which is now in closer agreement with the Compton et al.[1] value. Our calculations indicated the GEN1 basis set to provide a slightly better description of this system. The inherent multiconfigurational nature of CH_3NO_2 and $CH_3NO_2^-$ can be seen by considering RHF and ROHF weights in the CASSCF wave function given in Table 6. The GEN1 basis set again reproduces the aug-cc-pVTZ description at a lower cost. CASSCF data yield a negative electron affinity, which is significantly improved with MP2 dynamic electron correlation with our MCQDPT2 wave functions that show weights similar to the MS-CASPT2 calculations of Arenas et al.[14]

SS-MCQDPT2 calculations with the smaller 10 orbital CASSCF active space yields an electron affinity 0.02 eV larger than with 11 orbital's which represents the feasible limit at this time. Again, the GEN1 basis set reproduces the aug-cc-pVTZ value, which is in good agreement with the Compton et al.[1] value. A SS-MCQDPT2 reoptimization with 2×10^{-5} gradient threshold for the anion yields essentially no change to the reference geometry and nonoptimized energy, indicating the

TABLE 7: Calculated and Experimental Vertical Electron Affinities, EA_v, at the CH_3NO_2 Geometry, and Vertical Anion Detachment Energies (First Vertical Ionization Potential), DE_v, at the $CH_3NO_2^-$ Geometry[a]

level of theory	EA_v	DE_v
HFDFT(B3LYP)//6-311++G(2d,2p)[b]	N/A	1.214
B3LYP//aug-cc-pVTZ	−0.79[c]	1.152
mPW2PLYP//aug-cc-pVTZ	−0.353	0.878
mPW2PLYP//aug-cc-pVQZ	−0.324	0.849
MP2//aug-cc-pVTZ	−0.822	0.403
MP4SDQ//aug-cc-pVTZ	−0.516	0.842
CCSD//aug-cc-pVTZ	−0.375	0.950
CCSD(T)//aug-cc-pVTZ	−0.519	0.718
SS-MCQDPT2//GEN1	−0.733	0.780
3S-MCQDPT2//GEN1	−0.764	0.875
MS-CASPT2//ANO-L[d]	−0.40	N/A
dissociative electron detachment	−0.74	N/A
laser detachment photoelectron spectroscopy	N/A	−0.97

[a] All calculations assume the B3LYP//aug-cc-pVTZ geometry, with energies in eV. [b] Reference 2, EA_v not reported. [c] Reference 13, with 6-311++G(3df,3pd) basis set, aug-cc-pVTZ optimizes to the dipole-bound anion. [d] Reference 14, DE_v not reported.

anion B3LYP reference geometry to be reasonable. Addition of two, three, and seven further CASSCF reference configurations then show convergence to the Adams et al.[8] value, with the 7S-MCQDPT2 calculation within the limits of the small experimental error. A four-point third-order polynomial extrapolation of these data then yields a limiting value of 0.170 eV, which is again within the small experimental error. These MCQDPT2 data represent very comprehensive wave functions, and with multiconfigurational character properly treated, the convergence on further dynamic electron correlation is most likely real. In summary, for the adiabatic electron affinity, the Adams et al.[8] value appears to represent an accurate experimental determination, and the higher experimental set of electron affinities do not appear to be correct in the limit of accurate ab initio multireference wave functions.

C. Vertical Electron Affinity. As a cross-check, the vertical electron processes are also calculated. Photoelectron techniques generally involve formation of the neutral species by photoinduced electron detachment of the anion and are ideally suited to observation of vertical processes. The recent Adams et al. study for resolution purposes did not employ a photodetachment wavelength that would yield a full photoelectron spectrum scan; however, the Compton et al.[1] and recent Goebbert et al.[46] studies did employ appropriate wavelengths and determined the vertical detachment energy at the anion geometry to be 0.96 ± 0.01 eV. The experimental vertical electron affinity at the neutral geometry has also been reported at 0.72 eV (uncertainty predicted to be ≈±0.1 eV) by dissociative electron detachment methods.[47] We therefore report calculated vertical neutral electron affinity, EA_v, and vertical anion electron detachment energy, DE_v, in Table 7.

Vertical valence electron affinities (at the neutral geometry) are all negative or unfavorable, indicating a valence-bound anion is not formed at the neutral geometry, and the vertical detachment energies (at the anion geometry) are positive or unfavorable. The vertical detachment energy of the anion is alternatively known as the first vertical ionization potential of the anion at its optimized geometry. These two properties are reasonably different (≈0.25 eV) owing to the large tilt angle difference of the NO_2 group in optimized neutral and anion geometries; that is, these two vertical processes consider two quite different geometries. For the vertical electron affinity, mPW2PLYP and CCSD methods underestimate this by ≈50%. MP2 overestimates this value, while MP4SDQ and CCSD(T) yield almost identical underestimations of ≈25%. As expected for a vertical process, single-reference wave function methods appear inappropriate. MCQDPT values are in excellent agreement with experiment. The vertical anion electron detachment energies show trends similar to those of the adiabatic electron affinity calculations. MP2 and MP4SDQ underestimate, CCSD fortuitously calculates close to the experimental value, and CCSD(T) underestimates by ≈25%. The MCQDPT2 data, like for the adiabatic data above, show convergence to the experimental value, with a three-point extrapolation yielding a value of ≈0.96 eV. These data further confirm the requirement for multiconfigurational wave functions and the apparent convergence of our highest level of theory. A summary of the experimental data consistent with our calculations is given in Figure 3.

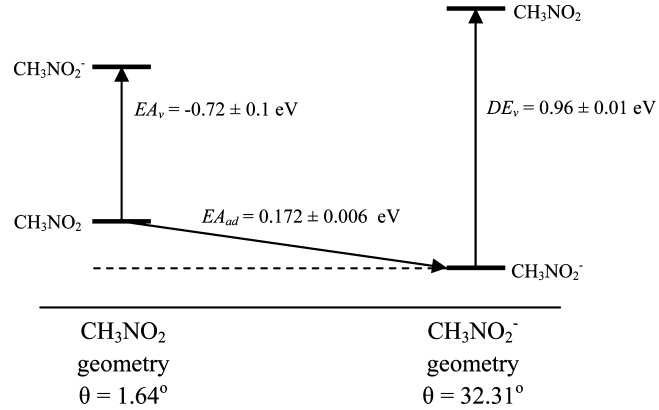

Figure 3. Summary of suggested experimental valence electron binding and detachment energies consistent with our reported MCQDPT2/B3LYP/GEN1 calculations.

D. Dipole-Bound Anion. The first reported experimental dipole-bound state binding energy, BE_D, of $CH_3NO_2^-$ was by Compton et al.[1] at 12 ± 3 meV, which also has been tentatively observed at 8 ± 8 meV by Adams et al.[8] The resonant electron-transfer experiments of Compton et al.[1] do generally show larger binding energies than other experimental methods and respective calculations.[48] Gutsev and Bartlett,[2] employing a Koopmans' theorem interpretation at the EA-EOM-CCSD/MP2/6-311++G(d,p)+7sp level of theory determined this to be 13 meV,[49] in apparent excellent agreement with experiment. Their additional diffuse functions were only of sp type with a geometric progression ratio of 2 that would promote basis set linear dependence problems. This same calculated binding energy was also earlier reported with ΔCCSD theory involving three additional sp diffuse functions augmented to a double-ζ quality valence basis set, and with Koopmans' theorem overestimating by ≈40% attributed to a poor dipole moment.[50] For dipole-bound anion determinations, description of molecular valence is less important than the dipole-bonding region since these two electronic configurations have little interaction. The Gutsev and Bartlett[2] dipole-binding study showed trends similar to that of the adiabatic electron affinity (Figure 2), that initial diffuse function (++) augmentation resulted in an ≈60% (6.1−14.4 meV) increase, with further polarization (2d,2p) yielding a slight decrease to apparent excellent agreement (12.7 meV) with experiment. Application of the 6-311++G(d,p)+7sp basis set yielded a slight increase to 13.3 meV, and still with the Compton et al.[1] experimental error. Such additional diffuse functions for other species with similar magnitude dipole moments are crucial for dipole-bound anions,[39,40] yet appeared to show intolerance in the EA-EOM-CCSD calculations. EA-EOM-CCSD (≈ΔCCSD level of theory)

TABLE 8: Calculated and Experimental $CH_3NO_2^-$ Dipole-Bound Anion Binding Energies, BE_D, in meV[a]

level of theory	BE_D
MP2/ACCD	4.8
CCSD/ACCD	7.9
CCSD(T)/ACCD	7.4
3S-MCQDPT/GEN1	8.9
resonant charge transfer[b]	12 ± 3
velocity map imaging[c]	8 ± 8

[a] ACCD = aug-cc-pVDZ+6sp7d with calculations assuming the B3LYP//aug-cc-pVTZ neutral geometry. [b] Reference 1. [c] Reference 8.

has been shown for O_3, which is isoelectronic to NO_2^-, to yield larger vertical valence electron affinities than EA-EOM-CCSDT with iterative triplets.[49] For valence effects, EA-EOM-CC methods do have the advantage of including some multiconfigurational character for an intrinsic type determination.[51] It has also been previously shown for a range of dipole-bound anions that ΔCCSD typically overestimates, while ΔCCSD(T) yields reasonable agreement.[39] All dipole-bound anion calculations here are again performed at the B3LYP//aug-cc-pVTZ geometry with any ΔZPV correction negligible. These calculations are summarized in Table 8. The experimental dipole moment of 3.46 D[52] is in good agreement with our B3LYP//aug-cc-pVTZ or GEN1 calculation, both at 3.60 D, and CASSCF(14,11)/aug-cc-pVTZ or GEN1, both at 3.43 D, and the CCD density at 3.63 eV with the aug-cc-pVDZ+6sp7d basis set.

These data reproduce the literature trend that ΔCCSD values appear to be slightly larger than ΔCCSD(T). The CCSD(T)/aug-cc-pVDZ+6sp7d calculation is smaller than the Compton et al.[1] value at 12 ± 3 meV, but in excellent accord with the value of Adams et al.[8] at 8 ± 8 meV, albeit larger error that includes the Compton et al.[1] value. Our calculations indicate the Gutsev and Bartlett[2] value of 13 meV warrants reinvestigation with a higher level of theory in basis set and electron correlation, as their agreement to the Compton et al.[1] value may again be fortuitous. Similar to EA-EOM-CCSD, analysis of 3S-MCQDPT2/B3LYP/GEN1 (without diffuse function augmentation) states yields a dipole binding energy of 8.9 meV.

The Adams et al.[8] study, consistent with a previous study by Lecomte et al.,[53] observed the dipole-bound state to disappear with argon solvation of the anion. To briefly qualitatively investigate this observation, we calculate for the $Ar.CH_3NO_2^-$ cluster at the MP2//aug-cc-pVDZ+6sp7d level of theory with a single Ar atom fixed at each end of the dipole, at a 3.5 Å separation with respect to the carbon or nitrogen. Counterpoise basis set superposition error corrections to the energies are included for Ar and CH_3NO_2 monomers. These binding energies are all strongly negative, on the order of ≈−900 meV and would indicate the dipole-bound state to disappear in the presence of single axial (3.5 Å) dipole solvation by argon. In accordance, the dipole-bound state appears to be an isolated phenomenon.

Conclusions

The reported calculations on the electron affinity of nitromethane demonstrate the difficulty of obtaining agreement between theory and experiment on a fundamental chemical molecular property, where both may be erroneous. We believe progress has been made on an accurate electron affinity determination for this species, and it has been demonstrated that ideally multiconfigurational wave functions are required to accurately describe the neutral and anion. Single-reference wave function calculations show some fortuitous or Pauling-point agreement, where cancellation of inadequate descriptions in basis set and/or electron correlation treatment may yield accidental agreement with a reported experimental value. The level of theory must be very carefully selected to accurately describe the system before any theoretical statements can be made on the accuracy of experimental data. By providing a systematic single and multireference study, convergence of our calculations supports the experimental value of 0.172 ± 0.006 eV to be consistent with theory, and the earlier and larger experimental determinations to be an overestimate. Are our calculations again in some fortuitous agreement? We believe this not to be the case; however, as a check, MR-CC or large scale MRCI calculations could be employed but at this time are considered far too expensive for the benefit. Present density functional theory (DFT) methods on first comparisons with some reported experimental electron affinities apparently appear to perform well but should be avoided for accurate energetic calculations involving anions from unphysical self-interaction. The double-hybrid mPW2PLYP and B2PLYP methods do appear to make a step toward an accurate description, where other methods incorporating full Hartree−Fock exchange significantly overestimate the adiabatic electron binding. B3LYP does provide very fast and accurate geometries. Our highest level of theory 3S-MCQDPT2 and 7S-MCQDPT2 with an aug-cc-pVTZ quality basis adiabatic values at 0.188 and 0.176 eV (0.170 eV extrapolated) respectively are assumed to be the best reported theoretical calculation so far, and we believe the ΔCCSD(T)/B3LYP/aug-cc-pVDZ+6sp7d dipole-bound state binding energy of 7−8 meV could be an improvement on previous EA-EOM-CCSD calculations employing poorer diffuse basis set description. We recommend use of the Adams et al.[8] value of 0.172 ± 0.006 eV as the molecular adiabatic valence electron affinity for nitromethane.

Acknowledgment. J.N.B. acknowledges financial support of a TEC Top Achiever scholarship. Computing facilities for GAMESS-US calculations were provided by the UCSC Blue-Fern (Blue Gene/L) facility. We thank the unknown referees for suggesting some alterations.

References and Notes

(1) Compton, R. N.; Carman, H. S., Jr.; Desfrançois, C.; Abdoul-Carime, H.; Schermann, J. P.; Hendricks, J. H.; Lyapustina, S. A.; Bowen, K. H. *J. Chem. Phys.* **1996**, *105*, 3472.
(2) Gutsev, G. L.; Bartlett, R. J. *J. Chem. Phys.* **1996**, *105*, 8785.
(3) Stockdale, J. A.; Davis, F. J.; Compton, R. N.; Klots, C. E. *J. Chem. Phys.* **1974**, *60*, 4279.
(4) Compton, R. N.; Reinhardt, P. W.; Cooper, C. D. *J. Chem. Phys.* **1978**, *68*, 4360.
(5) Chen, E. C. M.; Wentworth, W. E. *J. Phys. Chem. A* **1983**, *87*, 45.
(6) Grimsrud, E. P.; Caldwell, G.; Chowdhury, S.; Kebarle, P. *J. Am. Chem. Soc.* **1985**, *107*, 4627.
(7) Chen, E. C. M.; Welk, N.; Chen, E. S.; Wentworth, W. E. *J. Phys. Chem. A* **1999**, *103*, 9072.
(8) Adams, C. L.; Schneider, H.; Ervin, K. M.; Weber, J. M. *J. Chem. Phys.* **2009**, *130*, 074307.
(9) Gutsev, G. L.; Jena, P.; Bartlett, R. J. *J. Chem. Phys.* **1999**, *110*, 403.
(10) Oliphant, N.; Bartlett, R. J. *J. Chem. Phys.* **1994**, *100*, 6550.
(11) Blahous, C. P., III; Yates, B. F.; Xie, Y.; Schaefer, H. F., III. *J. Chem. Phys.* **1990**, *93*, 8105.
(12) Bera, P. P.; Yamaguchi, Y.; Schaefer, H. F., III; Crawford, T. D. *J. Phys. Chem. A* **2008**, *112*, 2669.
(13) Bull, J. N.; Maclagan, R. G. A. R.; Harland, P. W. *Mol. Phys.* **2009**, *107*, 1123.
(14) Arenas, J. F.; Otero, J. C.; Peláez, D.; Soto, J.; Serrano-Andrés, L. *J. Chem. Phys.* **2004**, *121*, 4127.
(15) Nguyen, M. T.; Le, H. T.; Hajgató, B.; Veszprémi, T.; Lin, M. C. *J. Phys. Chem. A* **2003**, *107*, 4286.
(16) Lykos, P.; Pratt, G. W. *Rev. Mod. Phys.* **1963**, *35*, 496.
(17) Davidson, E. R.; Borden, W. T. *J. Phys. Chem.* **1983**, *87*, 4783.

(18) Eisfield, W.; Morokuma, K. *J. Chem. Phys.* **2000**, *113*, 5587.
(19) Li, X.; Paldus, J. *Int. J. Quantum Chem.* **2009**, *109*, 1756.
(20) Sherrill, C. D.; Lee, M. S.; Head-Gordon, M. *Chem. Phys. Lett.* **1999**, *302*, 425.
(21) Manaa, M. R.; Freid, L. E. *J. Phys. Chem. A* **1998**, *102*, 9884.
(22) Arenas, J. F.; Centeno, S. P.; López-Tocón, I.; Pleáez, D.; Soto, J. *J. Mol. Struct. (THEOCHEM)* **2003**, *630*, 17.
(23) Manaa, M. R.; Freid, L. E. *J. Phys. Chem. A* **1999**, *103*, 9349.
(24) Arenas, J. F.; Otero, J. C.; Peláez, D.; Soto, J. *J. Chem. Phys.* **2003**, *119*, 7814.
(25) Arenas, J. F.; Otero, J. C.; Peláez, D.; J. Soto, J. *J. Chem. Phys.* **2005**, *122*, 084324.
(26) Zhu, R. S.; Lin, M. C. *Chem. Phys. Lett.* **2009**, *478*, 11.
(27) Finley, J.; Malmqvist, P.; Roos, B. O.; Serrano-Andrés, L. *Chem. Phys. Lett.* **1998**, *288*, 299.
(28) Gräfenstein, J.; Cremer, D. *Theor. Chem. Acc.* **2009**, *123*, 171.
(29) Zhao, Y.; Truhlar, D. G. *J. Phys. Chem. A* **2006**, *110*, 10478.
(30) Frisch, M. J.; Trucks, G. W.; Schlegel, H. B.; Scuseria, G. E.; Robb, M. A.; Cheeseman, J. R.; Montgomery, J. A., Jr.; Vreven, T.; Kudin, K. N.; Burant, J. C.; Millam, J. M.; Iyengar, S. S.; Tomasi, J.; Barone, V.; Mennucci, B.; Cossi, M.; Scalmani, G.; Rega, N.; Petersson, G. A.; Nakatsuji, H.; Hada, M.; Ehara, M.; Toyota, K.; Fukuda, R.; Hasegawa, J.; Ishida, M.; Nakajima, T.; Honda, Y.; Kitao, O.; Nakai, H.; Klene, M.; Li, X.; Knox, J. E.; Hratchian, H. P.; Cross, J. B.; Bakken, V.; Adamo, C.; Jaramillo, J.; Gomperts, R.; Stratmann, R. E.; Yazyev, O.; Austin, A. J.; Cammi, R.; Pomelli, C.; Ochterski, J. W.; Ayala, P. Y.; Morokuma, K.; Voth, G. A.; Salvador, P.; Dannenberg, J. J.; Zakrzewski, V. G.; Dapprich, S.; Daniels, A. D.; Strain, M. C.; Farkas, O.; Malick, D. K.; Rabuck, A. D.; Raghavachari, K.; Foresman, J. B.; Ortiz, J. V.; Cui, Q.; Baboul, A. G.; Clifford, S.; Cioslowski, J.; Stefanov, B. B.; Liu, G.; Liashenko, A.; Piskorz, P.; Komaromi, I.; Martin, R. L.; Fox, D. J.; Keith, T.; Al-Laham, M. A.; Peng, C. Y.; Nanayakkara, A.; Challacombe, M.; Gill, P. M. W.; Johnson, B.; Chen, W.; Wong, M. W.; Gonzalez, C.; and Pople, J. A. *Gaussian 03*, Revision C.02; Gaussian, Inc.: Wallingford, CT, 2004.
(31) Schmidt, M. W.; Baldridge, K. K.; Boatz, J. A.; Elbert, S. T.; Gordon, M. S.; Jensen, J. H.; Kosecki, S.; Matsunaga, N.; Nguyen, K. A.; Su, S. J.; Windus, T. L.; Dupuis, M.; Montgomery, J. A. *J. Comput. Chem.* **1993**, *14*, 1347.
(32) Zhao, Y.; Truhlar, D. G. *Theor. Chem. Acc.* **2008**, *120*, 215.
(33) Zhao, Y.; Truhlar, D. G. *Acc. Chem. Res.* **2008**, *41*, 157.
(34) Grimme, S. *J. Chem. Phys.* **2006**, *124*, 034108.
(35) Schwabe, T.; Grimme, G. *Phys. Chem. Chem. Phys.* **2006**, *8*, 4398.
(36) Nakano, H. *J. Chem. Phys.* **1993**, *99*, 7983.
(37) Hirao, K. *Chem. Phys. Lett.* **1993**, *201*, 59.
(38) Choe, Y.; Witek, H. A.; Finley, J. P.; Hirao, K. *J. Chem. Phys.* **2001**, *114*, 3913.
(39) Gutowski, M.; Skurski, P.; Jordan, K. D.; Simons, J. *Int. J. Quantum Chem.* **1997**, *64*, 183.
(40) Skurski, P.; Gutowski, M.; Simons, J. *Int. J. Quantum Chem.* **2000**, *80*, 1024.
(41) Shimanouchi, T. *J. Phys. Chem. Ref. Data* **1972**, *6*, 993.
(42) Ervin, K. M.; Ho, J.; Lineberger, W. C. *J. Phys. Chem.* **1988**, *92*, 5405.
(43) Milligan, D. E.; Jacox, M. E. *J. Chem. Phys.* **1971**, *55*, 3404.
(44) Gorse, D.; Cavagnat, D.; Pesquer, M.; Lapouge, C. *J. Phys. Chem.* **1993**, *97*, 4262.
(45) Gutsev, G. L.; Jena, P.; Bartlett, R. J. *Chem. Phys. Lett.* **1998**, *291*, 547.
(46) Goebbert, D. J.; Pichugin, K.; Sanov, A. *J. Chem. Phys.* **2009**, *131*, 164308.
(47) Walker, I. C.; Fluendy, M. A. D. *Int. J. Mass Spectrom.* **2001**, *205*, 171.
(48) Hammer, N. I.; Diri, K.; Jordan, K. D.; Desfrançois, C.; Compton, R. N. *J. Chem. Phys.* **2003**, *119*, 3650.
(49) Nooijen, M.; Bartlett, R. J. *J. Chem. Phys.* **1995**, *102*, 3629.
(50) Adamowicz, L. *J. Chem. Phys.* **1989**, *91*, 7787.
(51) Musiał, M.; Bartlett, R. J. *J. Chem. Phys.* **2003**, *119*, 1901.
(52) Lide, D. L. *CRC Handbook of Chemistry and Physics*; CRC Press: Cleveland, OH, 1996; Vol. 77, pp 10−214.
(53) Lecomte, F.; Carles, S.; Desfrançois, D.; Johnson, M. A. *J. Chem. Phys.* **2000**, *113*, 10973.

JP9113317